SCIENCE CHINA
Chemistry

• ARTICLES •

July 2015 Vol.58 No.7: 1169–1175
doi: 10.1007/s11426-015-5328-7

Efficiency enhancement of P3HT:PCBM polymer solar cells using oligomers DH4T as the third component

Ping Fu[1,3], Dong Yang[1,3], Fujun Zhang[2], Wei Yu[1,3], Jian Zhang[1*] & Can Li[1*]

[1] *State Key Laboratory of Catalysis; Dalian Institute of Chemical Physics, Chinese Academy of Sciences and Dalian National Laboratory for Clean Energy, Dalian 116023, China*
[2] *Key Laboratory of Luminescence and Optical Information, Ministry of Education, Beijing 100044, China*
[3] *University of Chinese Academy of Sciences, Beijing 100049, China*

Received September 4, 2014; accepted October 8, 2014; published online May 6, 2015

We assembled a ternary blend bulk heterojunction polymer solar cell (PSCs) containing P3HT (donor) and $PC_{61}BM$ (acceptor) incorporated with a small molecule oligomer, dihexyl-quaterthiophene (DH4T) as a third component. By optimizing the contents of DH4T, we increased the power conversion efficiency of ternary P3HT:DH4T:$PC_{61}BM$ PSCs to 4.17% from 3.44% of binary P3HT:$PC_{61}BM$ PSCs under AM 1.5 G of 100 mW/cm^2 intensity. The major improvement is from the increase of the short circuit current and fill factor that is due to the increased light absorption at short wavelength, the balanced charge carrier transportation and the enhanced hole evacuation by a DH4T-enriched layer at the anode interface. In this work, we demonstrated that the efficiency of the PSCs can be enhanced by using low-bandgap conjugated polymer and its oligomer as donors and fullerene derivatives as acceptors.

ternary polymer solar cells, P3HT:$PC_{61}BM$, oligomer, mobility, balanced charge carrier transportation

1 Introduction

Polymer solar cells (PSCs) have attracted more and more attention as a renewable energy source owing to their advantages of easy fabrication, low cost, light weight, and the possibility to fabricate flexible devices [1]. The system of P3HT: $PC_{61}BM$ PSCs was the mostly studied in the past ten years due to ease to processing and acceptable reproducibility, achieving power conversion efficiency (PCE) of 3%–5% [2,3]. The PCE of PSCs based on P3HT:$PC_{61}BM$ is mainly limited by the following factors: (1) a low short circuit current density (J_{sc}) and a low fill factor (FF) may result from the narrow absorption bands of P3HT and the unbalanced charge carrier transportation; (2) a low open circuit voltage (V_{oc}) is due to the large offsets of the energy levels of the highest occupied molecular orbital (HOMO) of P3HT and the lowest unoccupied molecular orbital (LUMO) of $PC_{61}BM$.

Different strategies have been carried out for tackling these restrictions in binary P3HT:$PC_{61}BM$ bulk heterojunction PSCs. Firstly, in order to improve J_{sc} and FF for achieving high performance PSCs, many research groups have committed to the synthesis of wide absorption bands polymer and adopting tandem structure to extend absorption range of the photoactive layer [4–8]. What's more, the balanced charge carrier transportation has been obtained by thermal annealing, synthesizing of high hole mobility materials and adjusting the blend ratios of donor and acceptor in bulk heterojunction PSCs [9–11]. Secondly, a series of fullerene derivatives with high LUMO energy levels have been synthesized to improve V_{oc} of the PSCs [12,13]. However, both synthesizing new materials and fabricating tandem PSCs have a lot of technical challenges and involve high cost. Therefore, we researched a novel device named ternary PSCs by introduction of an additional component. Ternary

---

*Corresponding authors (email: jianzhang@dicp.ac.cn; canli@dicp.ac.cn)

PSCs with a simple fabrication process are a promising candidate to extend the absorption spectra and to tune a suitable energy-level offset, which consequently lead to a larger J_{sc} and a higher V_{oc}, respectively [14–29]. Therefore, we presented a method by introduction of a p-type small molecule semiconductor into P3HT:PC$_{61}$BM as a ternary structure in order to tackle the two main limitations.

Oligomer DH4T has been studied extensively due to their unique electronic properties. It has been reported that DH4T was chosen originally in organic thin-film transistors (TFTs) as the double blend films with conjugated polymers for improving the hole mobility [30–33]. Compared with conjugated polymers, oligomers generally not only absorb short wavelength light, which is the complementary absorption of the P3HT:PC$_{61}$BM photoactive layer, but also possess high mobility for its strong tendency to form molecular crystals [34–37]. Particularly, the hole mobility of oligothiophenes, including DH4T, DH5T, and DH6T is up to 0.5 cm^2/(V s), much higher than that of polymer P3HT. Furthermore, oligomers have a monomer structure identical to polymer, so the soluble DH4T in organic solvents may eliminate the possible disorders and traps caused by molecules with other structures, such as dyes [38].

In this manuscript, we adopted a soluble high hole mobility p-type oligomer (DH4T) as the third component in P3HT: PC$_{61}$BM to balance the charge carrier transportation. To investigate the function of oligothiophenes DH4T, incorporation of different content of DH4T into P3HT: PC$_{61}$BM PSCs was studied as a model system for oligomer based ternary PSCs. The UV-Visible absorption, X-ray diffraction (XRD), carrier mobility estimated from space-charged-limited current (SCLC) method and the PSCs characterizations, showed that the DH4T as a third component in P3HT:PC$_{61}$BM, indeed, improves light harvesting at short wavelength and enhances the hole mobility, leading to a more balanced charge carrier transportation and a 21% improvement in PCE.

2 Experimental

2.1 Device fabrication

ITO substrates with a sheet resistance of 10 Ω/sq (Aim Core Technology Co. Ltd, Taiwan, China) were cleaned by sequential ultrasonic treatment in detergent, deionized water, acetone, isopropanol and ethanol, and then treated in an ultraviolet-ozone chamber for 15 min. Finally, they were transferred to a nitrogen-filled glove box. Branched polyethylenimine (PEI, Aldrich, USA) with a molecular weight of 25000 g/mol, was dissolved in methoxyethanol with a weight concentration of 0.05%. The solution was spin-coated onto the ITO substrate at a speed of 5000 r/min for 1 min and an acceleration of 1000 r/(min s), followed by annealing at 100 °C for 10 min on a hot plate. Subsequently, the active layer was prepared for the *o*-dichlorobenzene (*o*-DCB) solution of P3HT and PC$_{61}$BM (1:1, *w*/*w*, polymer concentration of 18 mg/mL, weight-averaged molecular weight, M_w<50000 g/mol, RiekeMetals Inc., Hong Kong, China) with/without (w/o) DH4T (blend weight ratios of DH4T/P3HT=5%, 8%, 10%, 15%) by spin-coating (1000 r/min, 30 s) on the ITO/PEI electrode. The films were dried in covered glass petri dishes for solvent annealing. A 15 nm MoO$_3$ layer and a 100 nm Ag layer were sequentially evaporated on the active layers as the anode in a vacuum chamber at a base pressure of 4×10^{-4} Pa.

2.2 Characterization

The current density-voltage (*J*-*V*) measurement of the PSCs was conducted on a computer-controlled Keithley 2400 Source Measure Unit (USA) under simulated AM 1.5 G irradiation (100 mW/cm^2) using a xenon-lamp-based OrielClass AAA solar simulator. External quantum efficiency (EQE) was characterized on the QTest Station 2000ADI system (Crowntech. Inc., USA). Atomic force microscopy (AFM) images were obtained using a Bruker Metrology Veeco Nanoscope III-D AFM (Germany). X-ray photoelectron spectroscopy (XPS) measurements were performed using a VG ESCALAB MK2 system with a monochromatized Al Kα under a pressure of 5×10^{-7} Pa. Transmission electron microscopy (TEM) images were obtained on a Hitachi instrument operated at 30 kV. High resolution transmission electron microscopy (HRTEM) images were obtained on a Tecnai G^2 F30 S-Twin (FEI Company) instrument operated at 300 kV. X-ray diffraction (XRD) patterns were recorded by Rigaku MiniFlex (Japan) diffractometer with a Cu Kα irradiation source at a speed of 1°/min. UV-Vis absorption spectra were recorded on a Varian Cary 5000 UV-Vis spectrophotometer (USA).

3 Results and discussion

Figure 1(a) illustrates the chemical structures of DH4T, P3HT and PC$_{61}$BM and the device configuration as follow: ITO/PEI/P3HT:DH4T:PC$_{61}$BM/MoO$_3$/Ag. Figure 1(b) illustrates the energy levels of P3HT, DH4T, and PC$_{61}$BM. DH4T has the intermediate energy levels between those of PC$_{61}$BM and P3HT, suggesting that photoexcited excitons might be dissociated efficiently and that the carriers can be efficiently driven forward until reaching the electrodes, which assist to better understand the role of DH4T in enhancing the V_{oc} [39].

Figure 2 shows typical *J*-*V* characteristics of the PSCs based on P3HT:PC$_{61}$BM and P3HT:DH4T:PC$_{61}$BM under AM 1.5 G illumination. The statistical J_{sc}, V_{oc}, FF, and PCE of the PSCs are listed in Table 1. For each type, more than 15 devices were fabricated. The P3HT:PC$_{61}$BM PSCs exhibited V_{oc} of 0.58 V, J_{sc} of 10.40 mA/cm^2, FF of 0.57 and PCE of 3.44%. The performance of the PSCs improved

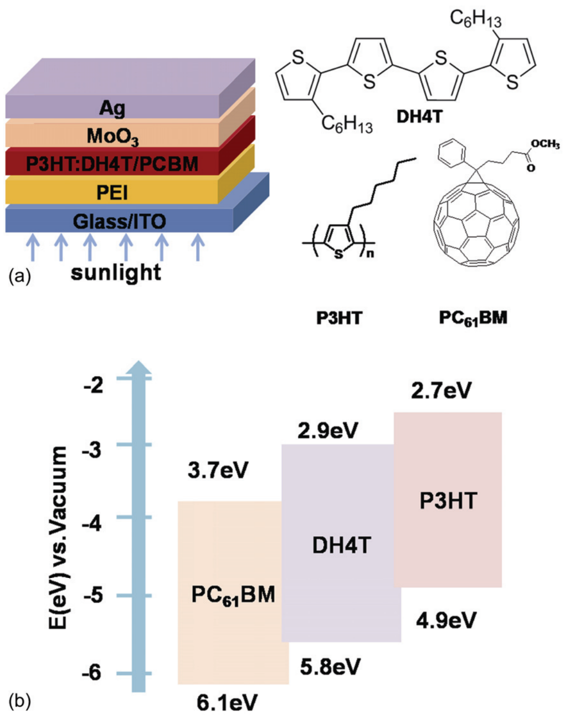

Figure 1 (a) The schematic configuration of the PSCs; (b) the highest occupied molecular orbital (HOMO) and lowest unoccupied molecular orbital (LUMO) energy levels of the materials in PSCs.

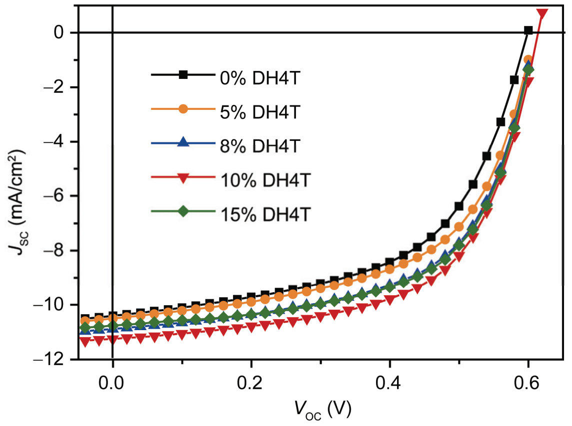

Figure 2 The *J-V* characteristics of the PSCs under AM 1.5 G illumination.

when the content of DH4T was increased until the weight ratio of 10% and then reduced by further increasing the DH4T content. The P3HT:DH4T:PC$_{61}$BM (1:0.1:1) PSCs exhibit J_{sc} of 11.21 mA/cm^2, V_{oc} of 0.60 V and FF of 0.62, yielding PCE of 4.17%, leading to a significant enhancement of 21% in PCE.

Obviously, the significant improvement can be attributed to the increase of the J_{sc} and FF. In the PSCs, J_{sc} and FF were generally affected by several factors such as light absorption, charge carrier transportation ability and interface properties. Figure 3(a) illustrates the EQE spectra of the PSCs. The P3HT:DH4T:PC$_{61}$BM (1:0.1:1) PSCs exhibited a response range from 350 to 650 nm, with a maximum EQE value of 68% at 520 nm. And then the EQE of devices decreased with a further increase of DH4T content, which was consistent with the measured J_{sc} in the corresponding PSCs. The variations between the integral values deduced from the EQE curves (9.1 mA/cm^2) and the measured values were similar to the results in literatures [11]. Compared with the binary P3HT: PC$_{61}$BM device, the ternary devices showed an improvement of EQE in the wavelength range 350–450 nm, corresponding to the absorption of DH4T because of its absorption band at 380 nm (Figure 3(b)), which means more efficient harvesting of photons in this range. Hence, the enhancement of absorbance at short wavelengths will contribute to the improvement of J_{sc}.

Futhermore, the electric neutrality during the whole photoelectric conversion process is a key factor for improving

Table 1 The parameters of the P3HT:PC$_{61}$BM PSCs and P3HT:DH4T:PC$_{61}$BMPSCs with different content of DH4T

P3HT:DH4T	J_{sc} (mA/cm^2)	V_{oc} (V)	FF	PCE (%)	μ_h (×10^{-4} cm^2/(V s))	μ_e (×10^{-4} cm^2/(V s))	μ_h/μ_e
1:0	10.40	0.58	0.57	3.44	1.17	3.82	0.31
1:0.05	10.50	0.60	0.58	3.65	1.92	3.68	0.52
1:0.08	10.84	0.60	0.61	3.97	1.95	3.63	0.54
1:0.10	11.21	0.60	0.62	4.17	3.18	3.56	0.89
1:0.15	10.76	0.62	0.59	3.94	3.73	3.02	1.24

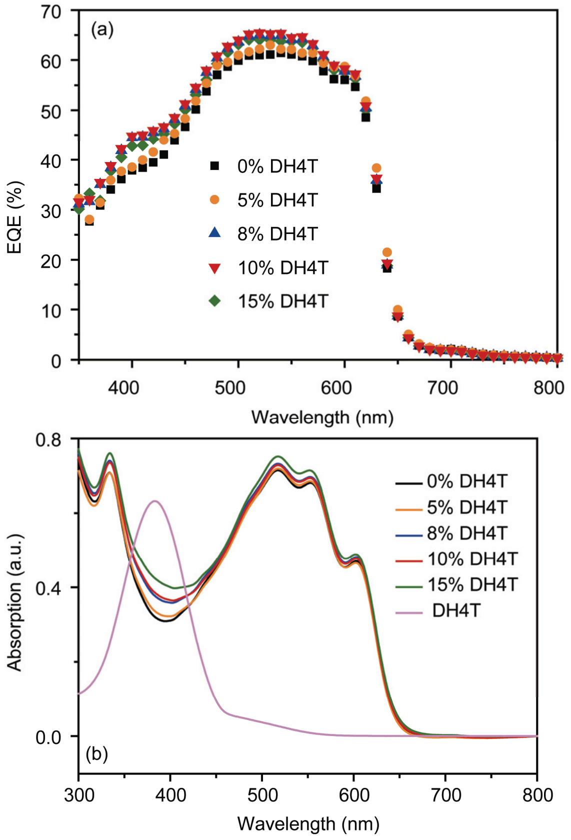

Figure 3 (a) The EQE curves of PSCs; (b) the absorption spectra of a P3HT:PC61BM film and P3HT:DH4T:PC61BM films with different content of DH4T (color online).

PSC devices. When the charge transport in the device is unbalanced (for example, in the pristine P3HT/PC$_{61}$BM system where μ_h is significantly lower than μ_e), hole accumulation occurs in the device, resulting in a loss in efficiency by increased recombination. To further investigate the dependence of the carrier mobility on the content of DH4T in the active layer, the carrier mobility was estimated by the space-charge-limited current (SCLC) model. The hole and electron mobility in P3HT:PC$_{61}$BM and P3HT:DH4T:PC$_{61}$BM PSCs are estimated for hole-only/electron-only devices. $J^{1/2}$-V curves of the hole-only devices (ITO/PEDOT:PSS/photoactive layer/MoO$_3$/Au) and the electron-only devices (ITO/PEI/photoactive layer/Ca/Al) in dark are shown in Figure 4.

In the trap-free region over the trap-filled limit, which is the limit of the presence of carrier traps, SCLC can be characterized by the Mott-Gurney square law [40], $J=(9/8)\varepsilon_r\varepsilon\mu_{h,e}(V^2/L^3)$, where ε is the vacuum permittivity, ε_r is the dielectric permittivity of the active layer, L is the thickness of the active layer, and $\mu_{h,e}$ is the hole or electron mobility, respectively. The hole and electron mobility of PSCs with different photoactive layers are listed in Table 1. It shows that the hole mobility increases with the increase of DH4T content. The electron mobility slightly decreases with an increased content of DH4T in the P3HT:DH4T:PC$_{61}$BM photoactive layers. The hole mobility and the electron mobility in the P3HT:DH4T:PC$_{61}$BM (1:0.1:1) PSCs are 3.18×10^{-4} and 3.56×10^{-4} cm^2/(V s), respectively, which are similar to (or slightly higher than) the values reported earlier for P3HT:PC$_{61}$BM blends [11] and the ratio between electron and hole mobility is close to unity ($\mu_h/\mu_e\approx0.89$), resulting in balanced carrier transport in the active layer. The balanced hole and electron transportation in P3HT:DH4T:PC$_{61}$BM (1:0.1:1) PSCs reduces the formation of space charges in devices, and that is beneficial for mitigating the charge recombination and a higher FF value of the corresponding PSCs is obtained, which agrees very well with the results by Hou *et al.* [41].

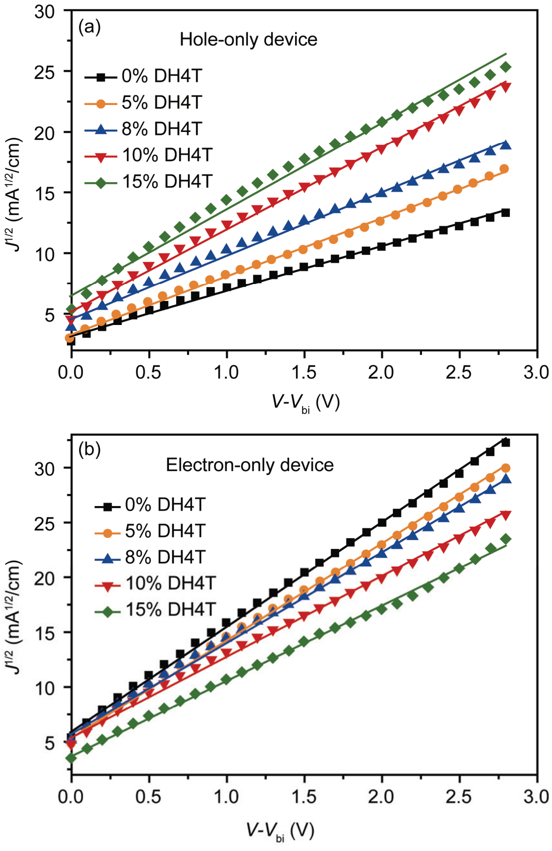

Figure 4 The $J^{1/2}$-V characteristics of hole-only devices (a) and electron-only devices (b).

Normally, the charge carrier transportation is dominated by the performance of the polymer and by the effects of crystals packing [42]. Therefore, we measured the XRD patterns of P3HT:PC$_{61}$BM and P3HT:0.1DH4T:PC$_{61}$BM films shown in Figure 5. A sharp diffraction peak at $2\theta\approx5.5°$ that corresponds to the (100) orientation of the P3HT crystallite was observed in the XRD spectra [43]. The P3HT:PC$_{61}$BM pristine film has a lower crystallinity. After the films introducing 0.1 wt% DH4T, the intensity of this main peak increased and the peak width at half-height decreased. These features show that the crystallinity of P3HT in the ternary composite films has been increased. A possible reason is that DH4T is used as crystallization nucleating agent in the photoactive layer of P3HT:PC$_{61}$BM [42].

The morphology of the active layer has been proved to play an important role in determining the device performance. TEM and AFM were used to investigate the effect of the DH4T on the phase-separation of the active layer. The topography and phase images by AFM of photoactive layers in PSCs are shown in Figure 6. The surface roughness of the P3HT:PC$_{61}$BM films was 2.78 nm, while the surface roughness of the P3HT:0.1DH4T:PC$_{61}$BM ternary films increased to 4.01 nm. The enlarged roughness of P3HT:DH4T:PC$_{61}$BM films can increase the contact area between the photoactive layer and the anode [44]. TEM

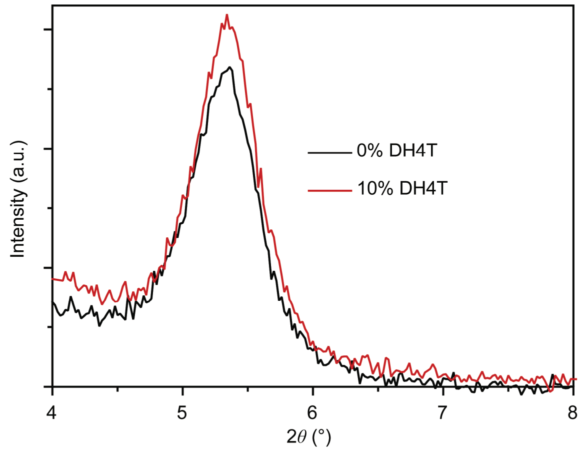

Figure 5 The XRD patterns of the P3HT:PC$_{61}$BM films and P3HT:DH4T:PC$_{61}$BM (1:0.1:1) films (color online).

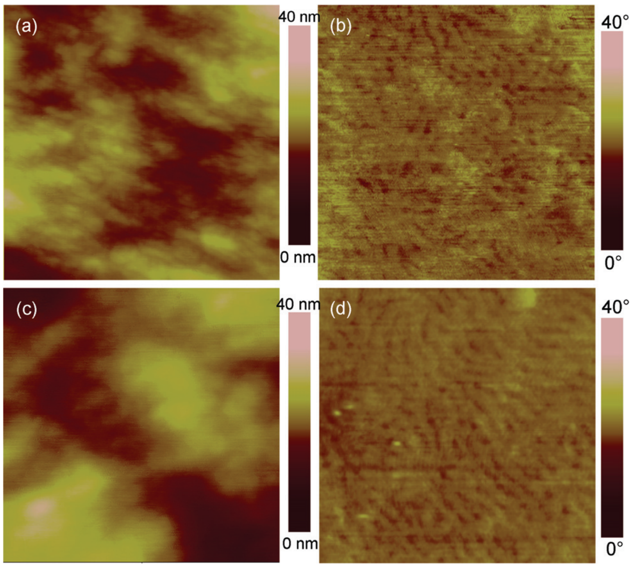

Figure 6 AFM topography and phase images of P3HT:PC$_{61}$BM films (a, b), P3HT:DH4T:PC$_{61}$BM (1:0.1:1) films (c, d) (color online). Scan size: 500 nm×500 nm.

images (Figure S1, Supporting Information online) correlate well with the phase images observed with AFM. After adding DH4T, the fibrillar-like P3HT crystals can be obviously observed in the donor/acceptor interpenetrating network within the composite film and the width of these fibrillar crystals was approximately 20 nm, which promotes efficient exciton charge dissociation and carrier transportation, to obtain higher J_{sc} and FF [45].

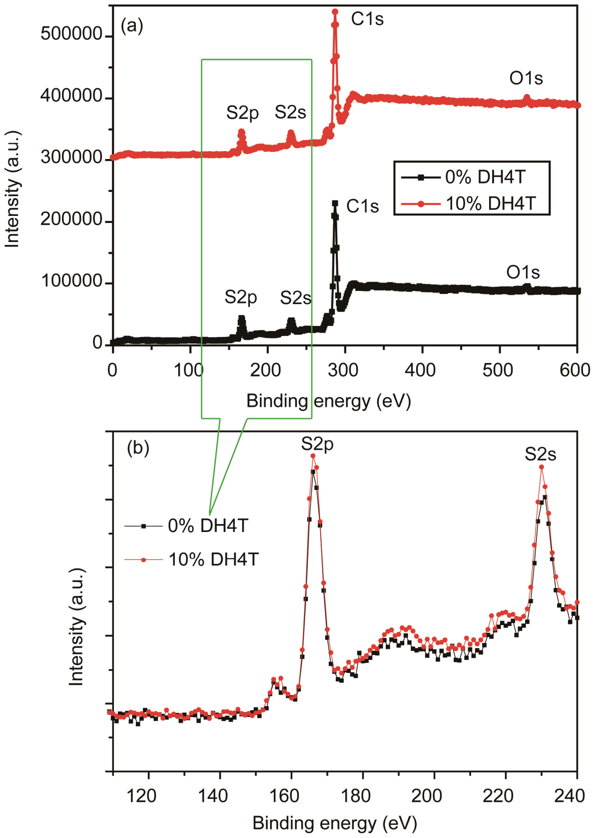

Figure 7 (a) The S2p, S2s, C1s and O1s XPS of the P3HT:PC$_{61}$BM PSCs and the P3HT:DH4T:PC$_{61}$BM (1:0.1:1) PSCs, respectively; (b) XPS spectra focusing on the S2p and S2s peaks.

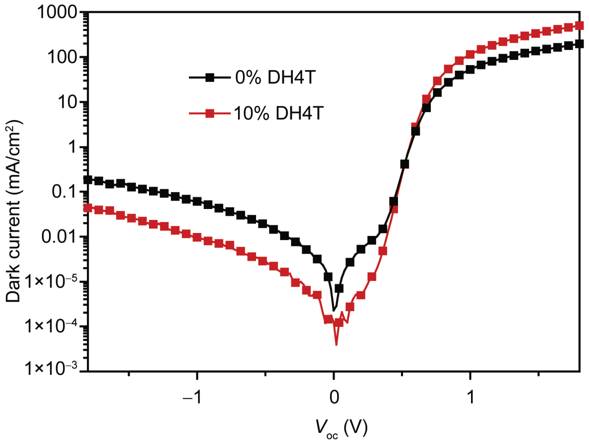

Figure 8 The *J-V* curves of the P3HT:PC$_{61}$BM PSCs and the P3HT:DH4T:PC$_{61}$BM (1:0.1:1) PSCs (color online).

Furthermore, the top surfaces of the P3HT:PC$_{61}$BM film and P3HT:DH4T:PC$_{61}$BM (1:0.1:1) film were characterized by XPS to determine the surface composition. The stoichiometric ratio of the components can be calculated directly from the peak intensities of individual elements [46]. In the P3HT:PC$_{61}$BM film, sulfur can be used as the characteristic element of the polymer because there is no sulfur in PC$_{61}$BM. Therefore, the weight ratios of PC$_{61}$BM to polymer at the top surfaces of the films can be evaluated using C/S atomic ratios obtained from the XPS measurement. The compositions of the P3HT:PC$_{61}$BM film and P3HT:DH4T:PC$_{61}$BM (1:0.1:1) film are provided in Figure 7. The measured atomic ratio of C1s and S2p peaks in the P3HT is 9.2, which is very close to the C/S stoichiometric ratio of 10, proving that the test is reliable. For the P3HT:PC$_{61}$BM film, P3HT:DH4T:PC$_{61}$BM (1:0.1:1) film and P3HT:DH4T film, the C/S ratios are 10.23, 9.84 and 7.67, respectively. And that the C/S stoichiometric ratio in DH4T is 7. Therefore, a lower C/S ratio is obtained after adding DH4T, which reveals that DH4T and P3HT chains enrich at the top of active layer while PC$_{61}$BM are present at the bottom of active layer in the inverted PSCs. As is well known, holes are transported to the anode along the network of electron donor materials while electrons are transported to the ITO cathode through the pathways of electron acceptor materials. Thus, electron donor and acceptor materials enriched at the top and bottom surface, respectively, which is favorable for charge carrier transport and will contribute to better device performance.

In the leakage dominated regime (<0.5 V), the dark current density of the P3HT:DH4T:PC$_{61}$BM (1:0.1:1) PSCs is apparently lower than that of the P3HT:PC$_{61}$BM PSCs

(Figure 8), the slightly increased V_{oc} may be attributed to the reduced leak current according to the Shockley equation [47].

4 Conclusions

In summary, we incorporated DH4T into P3HT:$PC_{61}BM$ as the third component of the PSCs. The PCE of P3HT:DH4T:$PC_{61}BM$ (1:0.1:1) PSCs increased to 4.17%, which is ~21% improvement in comparison with 3.44% of the P3HT:$PC_{61}BM$ PSCs. The improvement is attributed to the increased light absorption at short wavelength, the enhanced hole extraction by the DH4T-enriched layer at the anode interface and the balanced charge carrier transportation. Our results indicate that adding a solution-processed oligomer into polymer-based PSCs is an efficient method to further improve the performance of ternary PSCs.

Supporting information

The supporting information is available online at chem.scichina.com and link.springer.com/journal/11426. The supporting materials are published as submitted, without typesetting or editing. The responsibility for scientific accuracy and content remains entirely with the authors.

This work was financially supported by the National Natural Science Foundation of China (21374120). Jian Zhang acknowledges support by 100 Talents Program of the Chinese Academy of Sciences. The experimental characterization was supported by Pro. Xuming Wei and Pro. Mingrun Li.

1 Gunes S, Neugebauer H, Sariciftci NS. Conjugated polymer-based organic solar cells. *Chem Rev*, 2007, 107: 1324–1338

2 Li N, Stubhan T, Luechinger NA, Halim SC, Matt GJ, Ameri T, Brabec CJ. Inverted structure organic photovoltaic devices employing a low temperature solution processed WO_3 anode buffer layer. *Org Electron*, 2012, 13: 2479–2484

3 Dang MT, Hirsch L, Wantz G. P3HT:PCBM, best seller in polymer photovoltaic research. *Adv Mater*, 2011, 23: 3597–3602

4 Tan ZA, Li SS, Wang FZ, Qian DP, Lin J, Hou JH, Li YF. High performance polymer solar cells with as-prepared zirconium acetylacetonate film as cathode buffer layer. *Sci Rep*, 2014, 4: 4691

5 Zhang MJ, Guo X, Ma W, Ade H, Hou JH. A polythiophene derivative with superior properties for practical application in polymer solar cells. *Adv Mater*, 2014, 26: 5880–5885

6 Kim JY, Lee K, Coates NE, Moses D, Nguyen TQ, Dante M, Heeger AJ. Efficient tandem polymer solar cells fabricated by all-solution processing. *Science*, 2007, 317: 222–225

7 Zhang MJ, Gu Y, Guo X, Liu F, Zhang SQ, Huo LJ, Russell TP, Hou JH. Efficient polymer solar cells based on benzothiadiazole and alkylphenyl substituted benzodithiophene with a power conversion efficiency over 8%. *Adv Mater*, 2013, 25: 4944–4949

8 Tan ZA, Li LJ, Wang FZ, Xu Q, Li SS, Sun G, Tu XH, Hou XL, Hou JH, Li YF. Solution-processed rhenium oxide: a versatile anode buffer layer for high performance polymer solar cells with enhanced light harvest. *Adv Energ Mater*, 2014, 4: 1300884

9 Guo X, Zhang MJ, Cui CH, Hou JH, Li YF. Efficient polymer solar cells based on poly(3-hexylthiophene) and indene-C60 bisadduct fabricated with non-halogenated solvents. *ACS Appl Mater Interf*, 2014, 6: 8190–8198

10 Mihailetchi VD, Xie HX, de Boer B, Koster LJA, Blom PWM. Charge transport and photocurrent generation in poly (3-hexylthiophene): methanofullerene bulk-heterojunction solar cells. *Adv Funct Mater*, 2006, 16: 699–708

11 Li G, Shrotriya V, Huang JS, Yao Y, Moriarty T, Emery K, Yang Y. High-efficiency solution processable polymer photovoltaic cells by self-organization of polymer blends. *Nat Mater*, 2005, 4: 864–868

12 Guo X, Cui CH, Zhang MJ, Huo LJ, Huang Y, Hou JH, Li Y. High efficiency polymer solar cells based on poly(3-hexylthiophene)/indene-C-70 bisadduct with solvent additive. *Energ Environ Sci*, 2012, 5: 7943–7949

13 Zhang MJ, Guo X, Zhang SQ, Hou JH. Synergistic effect of fluorination on molecular energy level modulation in highly efficient photovoltaic polymers. *Adv Mater*, 2014, 26: 1118–1123

14 Hayashi Y, Sakuragi H, Soga I, Alexandrou I, Amaratunga GAJ. Bulk heterojunction solar cells based on two kinds of organic polymers and fullerene derivative. *Colloid Surface A*, 2008, 313: 422–425

15 Chen MC, Liaw DJ, Huang YC, Wu HY, Tai Y. Improving the efficiency of organic solar cell with a novel ambipolar polymer to form ternary cascade structure. *Sol Energ Mat Sol C*, 2011, 95: 2621–2627

16 Kim H, Shin M, Kim Y. Distinct annealing temperature in polymer: fullerene:polymer ternary blend solar cells. *J Phys Chem C*, 2009, 113: 1620–1623

17 Machui F, Rathgeber S, Li N, Ameri T, Brabec CJ. Influence of a ternary donor material on the morphology of a P3HT:PCBM blend for organic photovoltaic devices. *J Mater Chem*, 2012, 22: 15570–15577

18 Yuan K, Chen L, Chen Y. Photovoltaic performance enhancement of P3HT/PCBM solar cells driven by incorporation of conjugated liquid crystalline rod-coil block copolymers. *J Mater Chem C*, 2014, 2: 3835–3845

19 An QS, Zhang FJ, Zhang J, Tang WH, Wang ZX, Li LL, Xu Z, Teng F, Wang YS. Enhanced performance of polymer solar cells through sensitization by a narrow bandgap polymer. *Sol Energ Mat Sol C*, 2013, 118: 30–35

20 Khlyabich PP, Burkhart B, Thompson BC. Compositional dependence of the open-circuit voltage in ternary blend bulk heterojunction solar cells based on two donor polymers. *J Am Chem Soc*, 2012, 134: 9074–9077

21 Yang LQ, Zhou HX, Price SC, You W. Parallel-like bulk heterojunction polymer solar cells. *J Am Chem Soc*, 2012, 134: 5432–5435

22 Bechara R, Leclerc N, Leveque P, Richard F, Heiser T, Hadziioannou G. Efficiency enhancement of polymer photovoltaic devices using thieno-thiophene based copolymers as nucleating agents for polythiophene crystallization. *Appl Phys Lett*, 2008, 93: 013306

23 Honda S, Nogami T, Ohkita H, Benten H, Ito S. Improvement of the light-harvesting efficiency in polymer/fullerene bulk heterojunction solar cells by interfacial dye modification. *ACS Appl Mater Interf*, 2009, 1: 804–810

24 Honda S, Ohkita H, Benten H, Ito S. Multi-colored dye sensitization of polymer/fullerene bulk heterojunction solar cells. *Chem Commun*, 2010, 46: 6596–6598

25 Xu ZX, Roy VAL, Low KH, Che CM. Bulk heterojunction photovoltaic cells based on tetra-methyl substituted copper(II) phthalocyanine:P3HT:PCBM composite. *Chem Commun*, 2011, 47: 9654–9656

26 Peet J, Tamayo AB, Dang XD, Seo JH, Nguyena TQ. Small molecule sensitizers for near-infrared absorption in polymer bulk heterojunction solar cells. *Appl Phys Lett*, 2008, 93: 163306

27 Sharma SS, Sharma GD, Mikroyannidis JA. Improved power conversion efficiency of bulk heterojunction poly(3-hexylthiophene):PCBM photovoltaic devices using small molecule additive. *Sol Energ Mat Sol C*, 2011, 95: 1219–1223

28 Choi JW, Kulshreshtha C, Kennedy GP, Kwon JH, Jung SH, Chae M.

Solution-processed bulk heterojunction organic solar cells with high polarity small molecule sensitizer. *Sol Energ Mat Sol C*, 2011, 95: 2069–2076

29 Mikroyannidis JA, Tsagkournos DV, Sharma SS, Kumar A, Vijay YK, Sharma GD. Efficient bulk heterojunction solar cells based on low band gap bisazo dyes containing anthracene and/or pyrrole units. *Sol Energ Mat Sol C*, 2010, 94: 2318–2327

30 Russell DM, Newsome CJ, Li SP, Kugler T, Ishida M, Shimoda T. Blends of semiconductor polymer and small molecular crystals for improved-performance thin-film transistors. *Appl Phys Lett*, 2005, 87: 222109

31 Hwang DH, Kim SK, Park MJ, Lee JH, Koo BW, Kang IN, Kim SH, Zyung T. Conjugated polymers based on phenothiazine and fluorene in light-emitting diodes and field effect transistors. *Chem Mater*, 2004, 16: 1298–1303

32 Payne MM, Parkin SR, Anthony JE, Kuo CC, Jackson TN. Organic field-effect transistors from solution-deposited functionalized acenes with mobilities as high as 1 $cm^2/(V\ s)$. *J Am Chem Soc*, 2005, 127: 4986–4987

33 Wu YL, Li YN, Gardner S, Ong BS. Indolo[3,2-*b*]carbazole-based thin-film transistors with high mobility and stability. *J Am Chem Soc*, 2005, 127: 614–618

34 Garnier F, Hajlaoui R, El Kassmi A, Horowitz G, Laigre L, Porzio W, Armanini M, Provasoli F. Dihexylquaterthiophene, a two-dimensional liquid crystal-like organic semiconductor with high transport properties. *Chem Mater*, 1998, 10: 3334–3339

35 Halik M, Klauk H, Zschieschang U, Schmid G, Ponomarenko S, Kirchmeyer S, Weber W. Relationship between molecular structure and electrical performance of oligothiophene organic thin film transistors. *Adv Mater*, 2003, 15: 917–922

36 Paul KE, Wong WS, Ready SE, Street RA. Additive jet printing of polymer thin-film transistors. *Appl Phys Lett*, 2003, 83: 2070–2072

37 Lim E, Jung BJ, Chikamatsu M, Azumi R, Yase K, Do LM, Shim HK. Synergistic effect of polymer and oligomer blends for solution-processable organic thin-film transistors. *Org Electron*, 2008, 9: 952–958

38 Burke KB, Belcher WJ, Thomsen L, Watts B, McNeill CR, Ade H, Dastoor PC. Role of solvent trapping effects in determining the structure and morphology of ternary blend organic devices. *Macromolecules*, 2009, 42: 3098–3103

39 Huang JH, Velusamy M, Ho KC, Lin JT, Chu CW. A ternary cascade structure enhances the efficiency of polymer solar cells. *J Mater Chem*, 2010, 20: 2820–2825

40 Goodman AM. Double extraction of uniformly generated electron-hole pairs from insulators with noninjecting contacts. *J Appl Phys*, 1971, 42: 2823

41 Guo X, Zhang MJ, Tan JH, Zhang SQ, Huo LJ, Hu WP, Li YF, Hou JH. Influence of D/A ratio on photovoltaic performance of a highly efficient polymer solar cell system. *Adv Mater*, 2012, 24: 6536–6541

42 Mihailetchi VD, Wildeman J, Blom PWM. Space-charge limited photocurrent. *Phys Rev Lett*, 2005, 94: 126602

43 Chen TA, Wu XM, Rieke RD. Regiocontrolled synthesis of poly(3-alkylthiophenes) mediated by rieke zinc: their characterization and solid-state properties. *J Am Chem Soc*, 1995, 117: 233–244

44 Li G, Shrotriya V, Yao Y, Yang Y. Investigation of annealing effects and film thickness dependence of polymer solar cells based on poly(3-hexylthiophene). *J Appl Phys*, 2005, 98: 043704

45 Yang XN, van Duren JKJ, Rispens MT, Hummelen JC, Janssen RAJ, Michels MAJ, Loos J. Crystalline organization of a methanofullerene as used for plastic solar-cell applications. *Adv Mater*, 2004, 16: 802–806

46 Li H, Tang HW, Li LG, Xu WT, Zhao XL, Yang XN. Solvent-soaking treatment induced morphology evolution in P3HT/PCBM composite films. *J Mater Chem*, 2011, 21: 6563–6568

47 He C, Zhong CM, Wu HB, Yang RQ, Yang W, Huang F, Bazan GC, Cao Y. Origin of the enhanced open-circuit voltage in polymer solar cells via interfacial modification using conjugated polyelectrolytes. *J Mater Chem*, 2010, 20: 2617–2622